Arabian Journal of Geosciences (2021) 14:2087
https://doi.org/10.1007/s12517-021-08441-0

ORIGINAL PAPER

A thermo-hydraulic numerical model for the initial design of an underground thermal energy storage system in a coastal aquifer

Nihan Aydin Ertugrul[1] · Zubeyde Hatipoglu Bagci[2] · Ozgur L. Ertugrul[3]

Received: 18 March 2021 / Accepted: 9 September 2021

Abstract

Low entropy shallow ground heat resources are gaining importance in recent years owing to their availability compared to difficult-to-reach geothermal energy sources. In the last decades, aquifer thermal energy storage (ATES) systems have begun to be utilized increasingly since they can provide one of the cleanest and most energy efficient heating and cooling system alternatives for buildings. One of the main problems in the design phase of ATES systems is the correct estimation of thermal interference distance between extraction and injection side of the system. In order to investigate this problem, an extensive modeling study was carried out to constitute a preliminary approach for the numerical model calibration of heat transport and storage in aquifers. For this purpose, actual site data available for a well-studied coastal aquifer in Mediterranean region of Turkey was used in the analysis and performance assessment of a conceptual open-loop ground source heating well doublet. Three-dimensional coupled numerical model of groundwater flow and heat transfer was produced to constitute an approach for the thermo-hydraulic model calibration by estimating the duration of thermal breakthrough between the abstraction and injection wells. Simulation results were compared with the analytical solution for doublet well breakthrough time with finite hydraulic gradient. The comparison of results indicated that the numerical model is able to represent the thermal behavior in the field. Therefore, calibration methodology established in this paper could be followed in the pre-feasibility study and the design phase of low-temperature aquifer thermal energy storage systems worldwide.

Keywords Numerical modeling · Aquifer thermal energy storage · Thermal breakthrough · Analytical approach

Introduction

Techniques developed for the use of renewable energy resources have gained importance in recent years with the increase of awareness on environmental issues such as global warming, greenhouse gas emissions due to the consumption of fossil fuels, and excessive depletion of the Earth's resources (Rosen 1999). An increasing amount of research have been conducted to investigate the heat potential of shallow soils and aquifers in recent years (e.g., Andersson et al. 2003; Dickinson et al. 2009; Novo et al. 2010; Preene and Powrie 2009). Accordingly, **A**quifer **T**hermal **E**nergy **S**torage Systems (**ATES**), one of the versatile underground thermal energy storage methods, suggest a sustainable alternative for renewable energy supply (Bloemendal et al. 2015).The utilization of ATES technique contributes to reducing fossil energy consumption by providing a sustainable air conditioning alternative for buildings through seasonal heat storage (Cabeza et al. 2015; Kranz and Frick 2013).

ATES systems utilize low-temperature aquifer resources (Sanner 2001; Rafferty 2003). The basic working principle of the thermal energy storage technique in the aquifer is based on the principle of meeting the seasonal heat demand in buildings by making use of the heat potential of underground water

Responsible editor: Zeynal Abiddin Erguler

✉ Nihan Aydin Ertugrul
nihanertugrul@mersin.edu.tr

Zubeyde Hatipoglu Bagci
zubeyde@mersin.edu.tr

Ozgur L. Ertugrul
ozgurertugrul@hotmail.com

1 Directorate of Construction and Technical Works, Mersin University, 33343, Ciftlikkoy, Mersin, Turkey

2 Department of Geological Engineering, Mersin University, 33343, Ciftlikkoy, Mersin, Turkey

3 Department of Civil Engineering, Mersin University, 33343, Ciftlikkoy, Mersin, Turkey

Published online: 30 September 2021

temperatures that are not affected by climatic changes beginning from a depth of approximately 10 m from the surface (Banks 2012). For this purpose, in suitable aquifers, groundwater is extracted and injected at different entropies at two separate wells practically called as “hot” and “cold” wells. The heat energy available in the groundwater is gained by mechanical heat exchangers during the winter period and used for heating type air conditioning of the infrastructure, and then the lower temperature underground water is injected into another well at a suitable distance. In the summer, the waste and stored underground heat energy is re-used for the cooling type air conditioning of the buildings in winter period. The system is operated reversibly in cooling and heating periods for air conditioning purposes in residences, offices, etc. in cooling and heating periods to ensure sustainable air conditioning (Bloemendal and Hartog 2018).

The key challenge in the planning, installation, and operation of low-temperature ATES is to ensure a cost-effective as well as sustainable exploitation of the subsurface (Rostampour et al. 2016). An understanding of the thermo-hydraulic processes in the aquifer is necessary for the proper design of an ATES system under given hydrogeological and thermo-hydraulic conditions. In this study, field investigations such as groundwater level and temperature measurements have been carried out in the Karaduvar (Mersin-Turkey) coastal aquifer, which is thought to be suitable for thermal energy storage due to the relatively low natural groundwater velocity as stated in a study showing potential areas for different underground thermal energy storage system applications of Turkey (Cetin et al. 2020). Considering the field data obtained, groundwater flow is modeled with MODFLOW (Harbaugh et al. 2000) software, a finite difference code. Subsequently, thermo-hydraulic model taking into account the mechanisms of conductive and convective heat transfers and dispersion is modeled using MT3DMS (Harbaugh et al. 2000) software. By using numerical modeling technique, heat transfer scheme and the thermal response for the coastal aquifer are simulated. A three-dimensional coupled numerical model of groundwater flow and heat transfer is known to be an effective way to optimize and determine the sustainable development and utilization plan for aquifer thermal energy storage system. However, proper thermo-geological calibration of the three-dimensional numerical model for low-temperature heat transfer for shallow soil layers and aquifers plays a major role in the quality of the results. According to authors’ best knowledge, there is not any available study concentrating on the calibration of the thermo-geological model. The objective of this study is therefore to constitute an approach for the numerical model calibration by comparing the temperature values produced by the finite difference thermo-hydraulic model with the analytical solution of the temperature field inside the aquifer.

Literature review on the design of ATES systems

Heat energy can be stored in shallow geological formations. Temperatures underground, from a depth of about 10 m, become stable throughout year, not being affected by seasonal temperature changes (Banks 2012). Underground thermal energy storage solutions can be applied with different techniques (Fleuchaus et al. 2018). ATES technique is considered as one of a number of subsurface techniques that use the shallow geological strata and aquifers as a warm or cold water storage medium. Other forms of thermal mass storage include pit storages, rock-caverns, closed loop pipes, duct or borehole systems in unconsolidated materials or solid rock, and open-loop gravel-water pit storages (Bridger and Allen 2005). A schematic representation of the ATES technique (Schüppler et al. 2019) is illustrated in Fig. 1.

Aquifer thermal energy storage technique is particularly suitable to store large amounts of thermal energy (Sommer et al. 2013). The system has developed into a cost-effective alternative for heating and cooling of residential and utility buildings such as commercial offices, hospitals, dormitories, universities, and greenhouses. Moreover, these systems reduce greenhouse gas emissions by replacing fossil fuel based heating and cooling systems (Cetin et al. 2012). Although utilization of aquifer thermal energy storage systems relies on the presence of suitable aquifers at the site, they have lower initial drilling and equipment expenditures compared to closed loop borehole thermal energy storage (BTES) systems (Lee 2013).

The amount of energy that could be recovered from the aquifer is generally lower than the amount that is stored because part of the injected energy is lost due to dissipation of heat to the surroundings of the storage and advection with regional groundwater flow. The efficiency of the ATES technique is generally measured by the thermal recovery ratio parameter, which indicates how much of the stored heat energy can be recovered after a certain period of time (Sommer et al. 2013). Thermal recovery ratio is influenced by hydrogeological, design-specific, and anthropogenic factors. In a previous numerical modeling study on the thermal efficiency of ATES systems, it has been shown that with the increase of groundwater velocity, heat losses increase due to the dissipation of the stored thermal energy in the aquifer (Groot 2013). For this reason, determining the presence of a suitable aquifer for heat recovery plays an important role in the first step of the system design. In general, suitable aquifers can easily supply sufficient amount of groundwater to the system. Groundwater must have a relatively low hydraulic gradient and therefore a low flow velocity so that the stored heat does not dissipate and be transported from the storage area of the well. For this reason, the groundwater flow velocity and direction should be taken into consideration in the planning and design stage of an ATES system. In addition, the heating of groundwater may negatively affect thermal energy

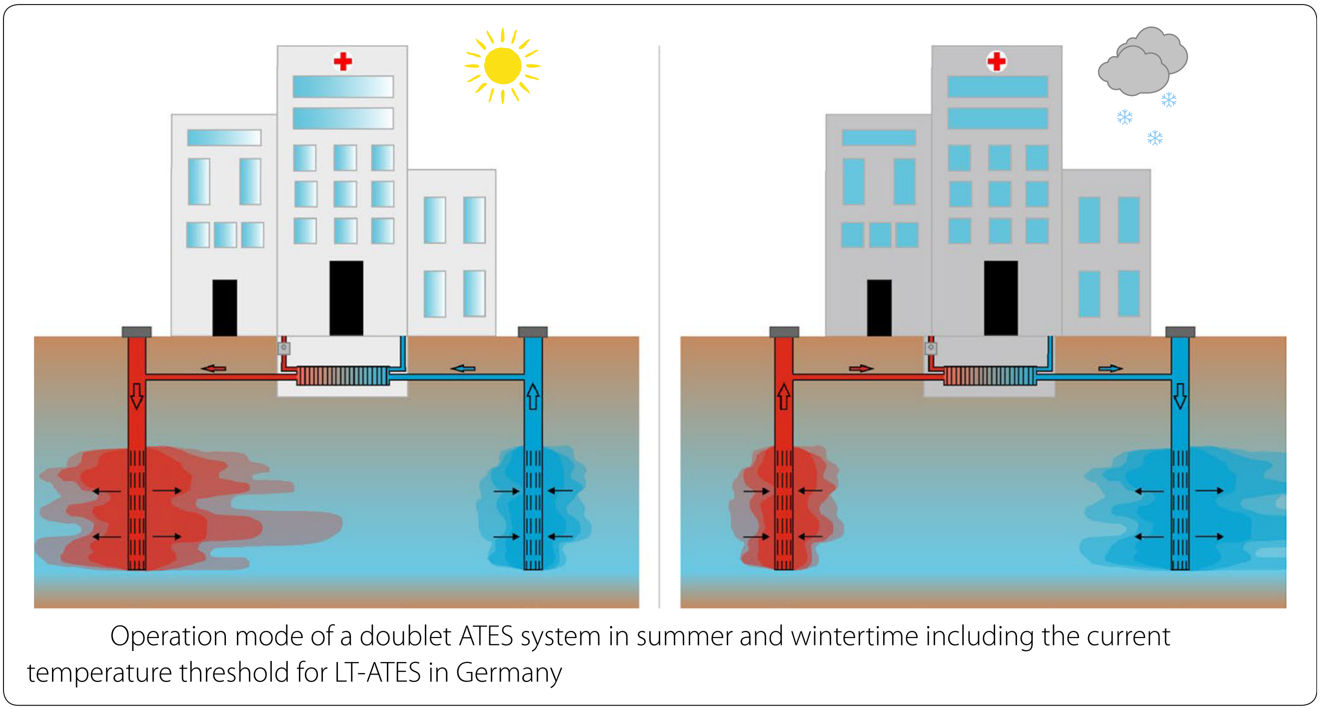

Fig. 1 Seasonal working principle of a doublet type ATES system (Schüppler et al. 2019)

storage efficiency by causing changes in water density and viscosity (Hecht-Méndez et al. 2010). Hence hot water is stored at most 5 °C above the average temperature of the aquifer (Dickinson et al. 2009; Lee 2010; Gao et al. 2017) at present study. In addition, buoyancy flow was ignored in this study because at the relative small temperature differences between the wells and ambient groundwater as applied for ATES, buoyancy effects are negligible (Bloemendal and Hartog 2018; Anderson 2005; Doughty et al. 1982).

Hydraulic and thermal breakthrough between abstraction and injection wells

One of the most important factors ruling the design of the thermal energy storage system in the aquifer is the thermal radius parameter. The heat migration rate in the groundwater environment is generally less than the groundwater flow velocity. Assuming that the volume of groundwater injected back into the underground heat reservoir by ATES wells has a cylindrical geometry in homogeneous and isotropic environments (Fig. 2), hydraulic radius (R_h) can be determined by Eq. (1). By using Eq. (2), a thermal radius distance can be determined between wells that will prevent thermal interference which may occur between abstraction and injection wells, as well as providing balance in terms of hydraulic feedback. In Eq. (2), c_w and c_a denote the specific heat capacities of groundwater and aquifer (J/kg K), V is the total volume of water abstracted or injected in a period (m^3), and H is the length of the well filter (m). Researchers offer different opinions on thermal interaction distances between wells. Based on the results of numerical modeling studies, Kim et al. (2010) stated that the thermal recovery rate in ATES systems is not

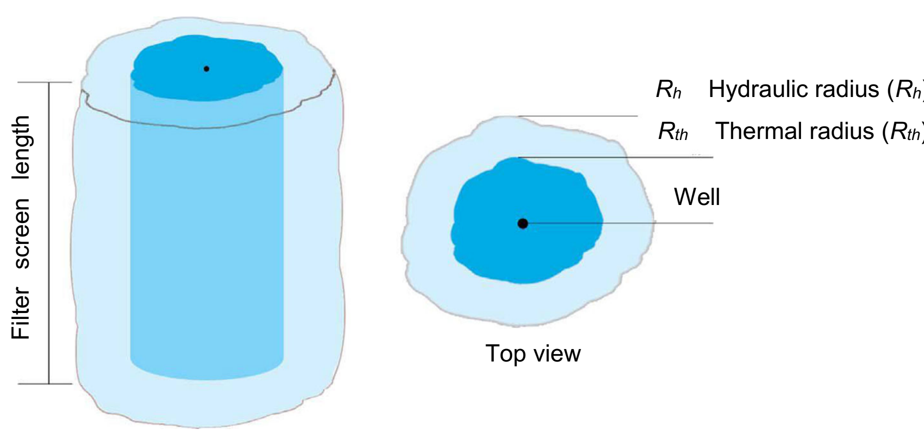

Fig. 2 Representation of thermal and hydraulic radius of an ATES well in homogeneous and isotropic aquifer conditions (Bloemendal 2018)

significantly affected if the distance between abstraction and injection wells is more than one thermal radius. Sommer et al. (2015) stated that thermal recovery will decrease if the distance between wells is less than two thermal radii. The Netherlands Underground Heat Storage Organization (NVOE 2006) recommends that the distance between wells should be at least three thermal radii to avoid thermal interference.

$$R_\mathrm{h} = \sqrt[2]{\frac{V}{n\pi H}} \tag{1}$$

$$R_\mathrm{th} = \sqrt[2]{\frac{c_\mathrm{w}V}{c_\mathrm{a}\pi H}} \tag{2}$$

The minimum distance L(m) to prevent hydraulic feedback between the abstraction and injection wells can be determined by Eq. (3) as suggested by Banks (2012). Here, Q (m^3/s) is abstraction/injection flow rate, T (m^2/s) is the transmissivity of the aquifer given in Eq. (4) which is the multiplication of the hydraulic conductivity (K) by the aquifer thickness (b), and i is the hydraulic gradient. As expressed with Eq. (5), when minimum distance (L) is included in the denominator part, the equation is converted to another coefficient, namely β. When this coefficient becomes greater than one, the probability of injected groundwater being pumped out by the extraction well increases (Banks 2012).

$$L = \frac{2Q}{\pi Ti} \tag{3}$$

$$T = b \cdot K \tag{4}$$

$$\beta = \frac{2Q}{\pi TiL} \tag{5}$$

The time it takes for groundwater to travel from the injection well to the abstraction well is defined as the hydraulic breakthrough time (Banks 2012). The hydraulic breakthrough time (t_hyd) can be calculated by Eq. (6) for the cases where hydraulic gradient exists. On the other hand, heat migration in the groundwater environment is not prompt and thermal equilibrium in the aquifer matrix is not reached in short time. In a groundwater aquifer, heat transport occurs by three mechanisms (Banks 2012). First mechanism is heat conduction occurring through mineral grains and water-filled pores; second mechanism is the advection with bulk groundwater flow and third mechanism is the exchange between moving groundwater and the aquifer matrix composed of solid material and immobile pore water.

To assess the risk of thermal breakthrough, abstraction well is located directly up-gradient of the injection well as illustrated in Fig. 3 a (Banks 2015). Equation (7) gives the thermal breakthrough time (time for the transport of heat back to the abstraction well, t_the) in a well doublet if the initial regional natural hydraulic gradient is finite (Clyde and Madabhushi 1983; Banks 2011). This equation obeys Darcy's law and based on the assumption that the aquifer is a homogeneous and saturated porous medium and instantaneous thermal equilibrium is valid (de Marsily 1986). In Eq. (6) and Eq. (7), L is the distance between well doublet, n is the porosity of the aquifer, K is the hydraulic conductivity of the aquifer, and $c_\mathrm{aq,\ v}$ and $c_\mathrm{w,\ v}$ are the specific volumetric heat capacities of the saturated aquifer (i.e., mineral matrix plus pore water) and groundwater respectively. It should also be noted that this equation does not account for dispersion effects

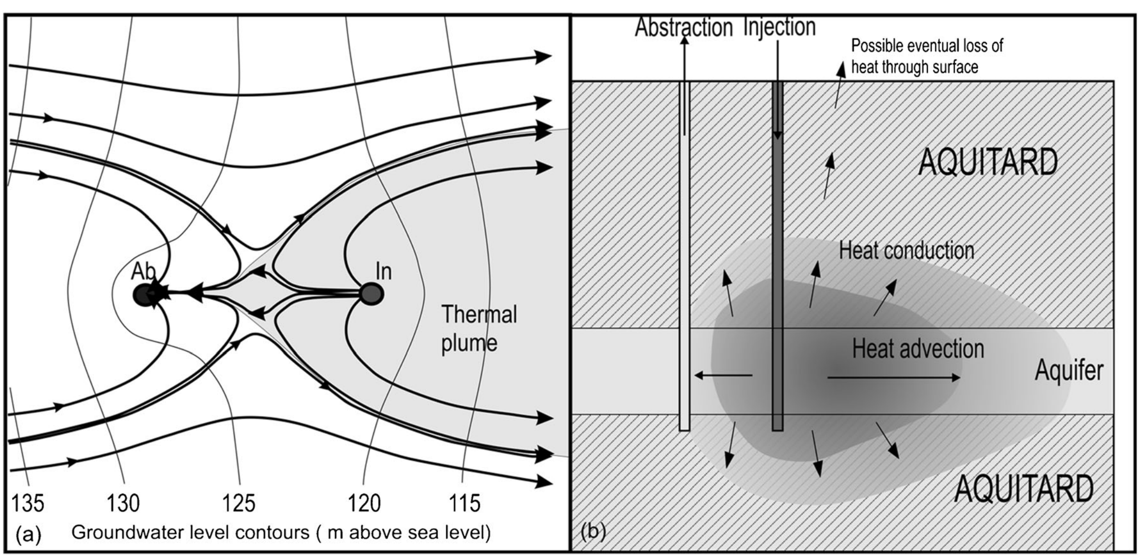

Fig. 3 A well doublet system, consisting of an abstraction well, situated immediately up the hydraulic gradient from an injection well. **a** The shaded area showing the thermal plume and **b** a section showing the heat loss by conduction into over and underlying rocks (Banks 2015)

and assumes there is no vertical conduction of heat to overlying or underlying strata as illustrated in Fig. 3 b since the heat fluxes are treated as totally two dimensional. However, three-the dimensional finite difference numerical modelling work suggests that the vertical conduction of heat away from the aquifer is always significantly important for the heat balance around a well doublet, effectively retarding the lateral migration of heat further hence restricting lateral thermal plume development (Banks 2015).

$$t_{\mathrm{hyd}} = \frac{Ln}{Ki}\left[\frac{\beta}{\sqrt{\beta-1}}\tan^{-1}\left(\frac{1}{\sqrt{\beta-1}}\right)-1\right] \tag{6}$$

$$t_{\mathrm{the}} = \frac{Lc_{\mathrm{aq,v}}}{c_{\mathrm{w,v}}Ki}\left[\frac{\beta}{\sqrt{\beta-1}}\tan^{-1}\left(\frac{1}{\sqrt{\beta-1}}\right)-1\right)\right] \tag{7}$$

Study area

Location, climate, hydrology, and hydrogeology

The site selected for the conceptual ATES system simulation carried out in this study is located within the boundaries of the Mediterranean Municipality of Mersin and completely includes the neighborhood of Karaduvar district. A preliminary field study was carried out in the eleventh month of 2018 in order to determine the existing wells that will allow the measurement of the groundwater level in the Karaduvar district and to determine the extent of the area suitable for thermal energy storage. The borehole log data of the wells drilled by the State Hydraulic Works Department of Turkey (DSİ) in the vicinity of Karaduvar Region was used within this research. Most of the location data related with these boreholes were obtained from a previous study conducted by Hatipoglu-Bagci(2004). Based on the data gathered from the existing well logs, an area of 1 km × 1 km around the State Hydraulic Works Borehole (#8178) is thought to be suitable in terms of geological formations to store heat energy (Fig. 4). Since the groundwater hydraulic gradients are relatively low in this selected area, it is predicted that the efficiency of the conceptual ATES system will be higher in this zone.

The study area is located in the southern part of the 1/25,000 scale Mersin land register map (#O33-a3) and is in the proximity of Deliçay River and Mersin Free Trade and Customs Zone in the east-west direction, and by the Mersin-Adana state highway (D400) and the Mediterranean sea in the north-south direction. Study area, shown in Fig. 4, takes place between the coordinates of 650000-651000 in the X direction and 4075000-4076000 in the Y direction according to UTM ED50 system.

Study area is located in a low-lying coastal plain formed by a deltaic environment. Quaternary age uncemented granular units form a productive coastal aquifer in this area (Hatipoglu-Bagci et al. 2019). The stratigraphic profile of the underground is idealized by using the borehole log data obtained from General Directorate of State Hydraulic Works(DSİ). The locations of DSI-well logs nearby the study area in the Mersin-Karaduvar region are also depicted in Fig. 4. Idealized soil profile of the study area is depicted in Fig. 5. The thickness of gravel layer containing clay grains ranges approximately from 23.00 to 25.00 m. Monthly average total precipitation amount (mm) and average temperature (°C) values for the year 2019 were obtained from Turkish State Mersin Meteorological Service Agency. According to 2019 data, the highest rainfall in Mersin Province was measured as 261 mm in January and the least precipitation was recorded as 2.1 mm in May. Total precipitation was obtained to be 846.5 mm for the year of 2019. Temperature data given in Fig. 6 is the average of temperature values measured between 1940 and 2019 in Mersin Province.

Observation wells

The existence of a large number of pump-type irrigation wells with a depth varying between 10 m and 20 m was observed in the vicinity of the study area. The availability of sufficient wells for measurements in the field has provided an important convenience in collecting the required data. Well locations and top elevations of the terrain were determined using GPS-based location determination device. In order to represent the groundwater system for a whole year in a steady-state condition and to determine the average groundwater temperatures, measurements were carried out in the study area between years 2018–2019. Groundwater and temperature levels were monitored at the end of the dry seasons of each year, on dates 23.11.2018 and 30.11.2019.

Materials and method

Hydrogeological model

Since numerical simulation is a viable tool for understanding and predicting the behavior of complex systems, it can readily be used to assess the feasibility of an anticipated ATES system, while helping in the aquifer storage design and optimization of well locations. In the first step of this study, MODFLOW 8.0 software (Harbaugh et al. 2000) was used in the conceptualization of groundwater flow model. MODFLOW is a software developed to simulate groundwater flow under saturated flow conditions, where the groundwater

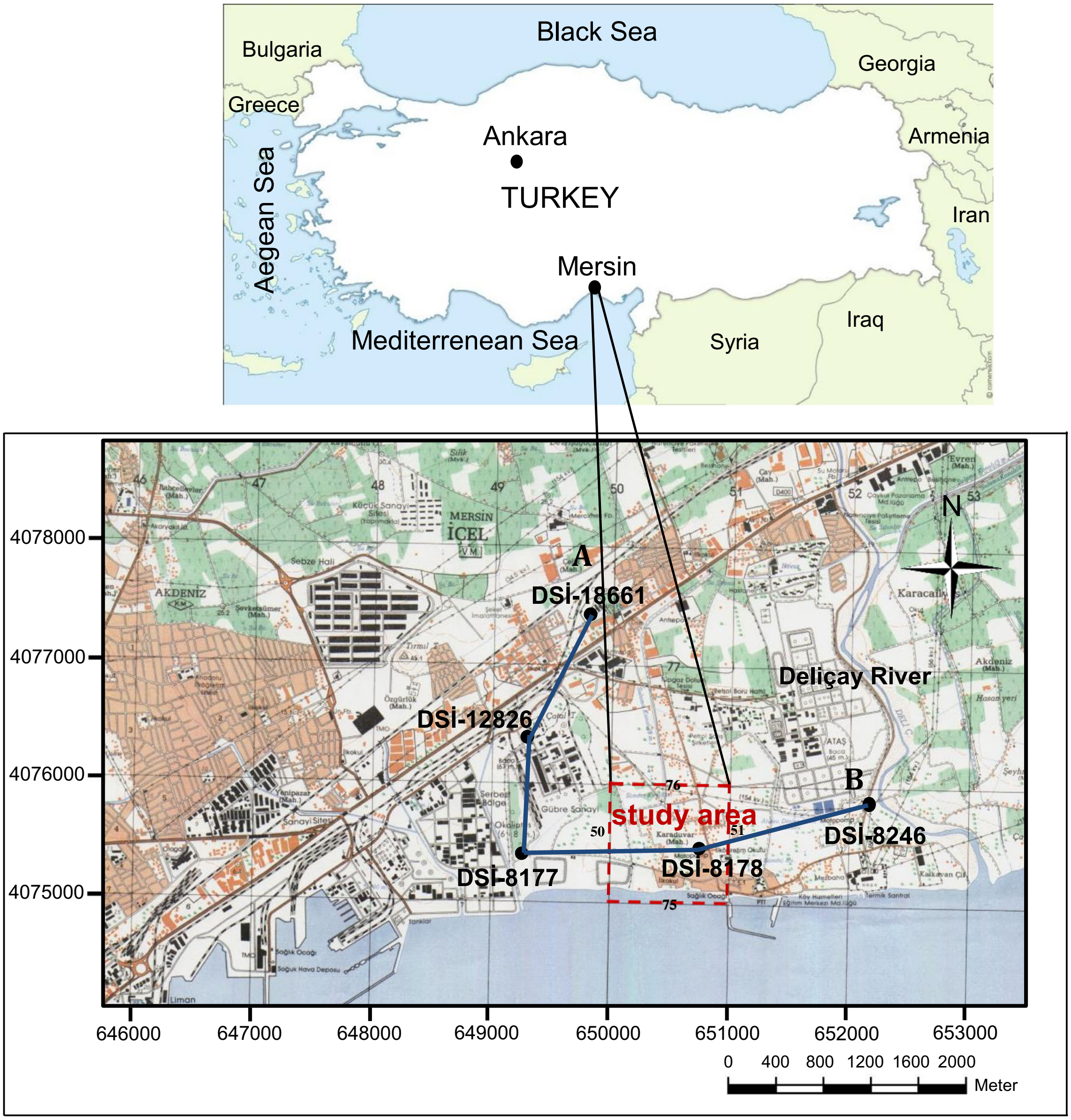

Fig. 4 Plan view of the study area,:(A, B) stratigraphic line and the location of State Hydraulic Works (DSİ) observation wells

density and hydraulic conductivity are considered constant and Darcy's law is valid.

Grid construction

For the conceptualization the coastal aquifer, the study area is discretized with 100×100 grid cells where the size of each cell has been determined as 10m × 10m. The upper topography data of the groundwater flow model were obtained through Surfer 12 software, which distributes the elevation values in irregularly spaced coordinates to the entire numerical model domain by the Kriging interpolation method. In order to set up the numerical model domain of the study area, the coordinate and elevation values (x, y, z) of a total of 510 points in the study area on the 1/25,000 scale map obtained from Mersin Provincial Directorate of Environment and Urbanization were used. These values were calculated by using Kriging interpolation method at each node using Surfer 12 program and turned into a text file in ASCII format. The soil layers in the model were defined as three different layers in line with the given stratigraphic profile (Fig. 4). Accordingly, the top layer is idealized as a low permeable clay layer with silt content, the second layer as a permeable gravel layer with clay content, and the third layer as a low permeable clay with gravel content. The lower and upper elevation values of each layer were estimated using the Kriging interpolation method. The depth of the model was defined as 100 m in the vertical (k) direction. Upper layer is defined as an unconfined aquifer while the underlying layers are defined as confined aquifer.

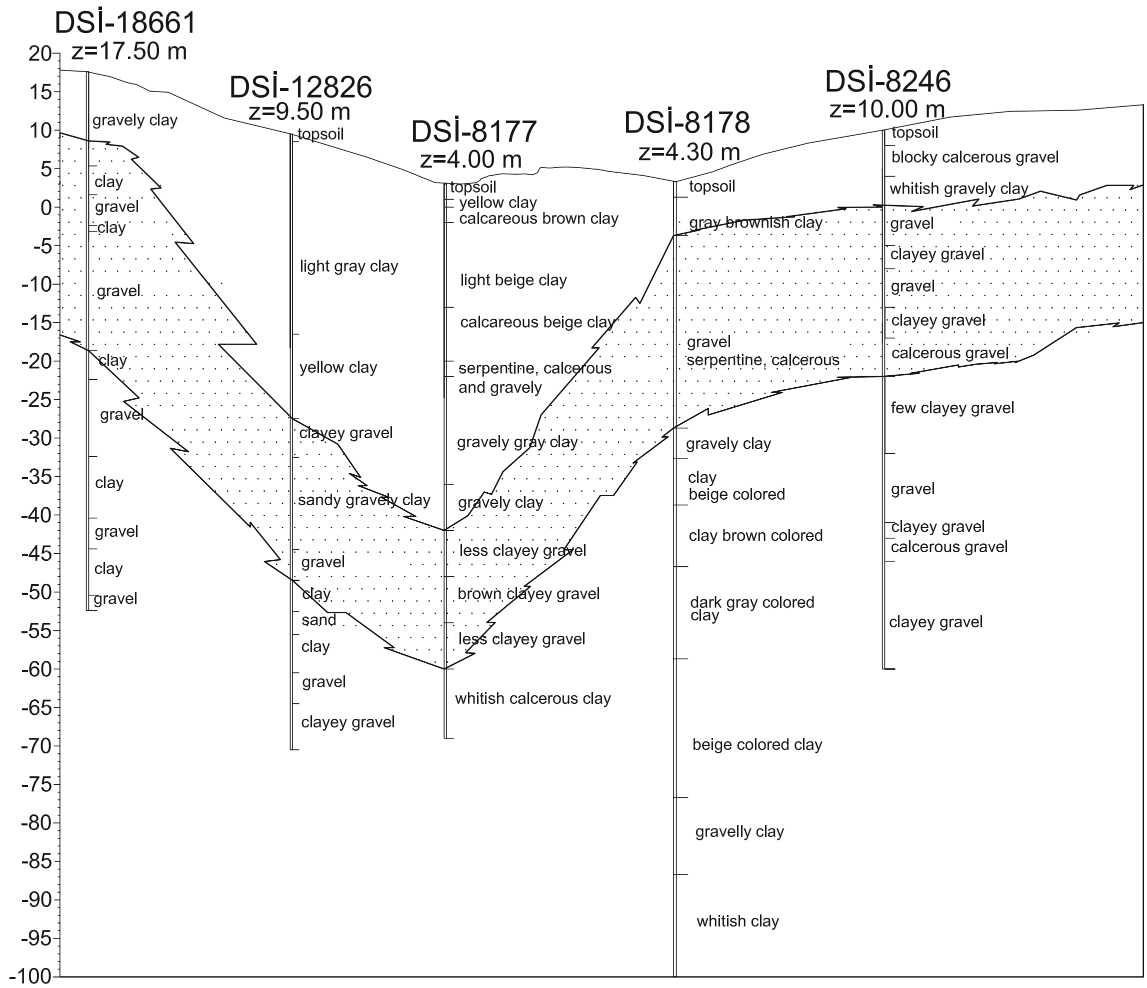

Fig. 5 (A, B) Line stratigraphic profile

Boundary conditions

In this study, the northern and southern boundaries of the 3D model domain were defined as constant head boundaries, whereas the other cells in the study area were attributed as active cells. A no-flow boundary condition for the model bottom was assumed. The values of the constant hydraulic head cells located in the northern edge of the study area were determined based on the groundwater level measurements performed in 2018. For the coastal boundary condition located on the southern boundary, hydraulic head values were adjusted to encounter the seawater pressure. Equivalent freshwater heads were computed by Eq. (8) suggested by Bear 1979. In this formula, h_f is equivalent freshwater head (L);h is head (L); ρ_f is density of freshwater (ML^{-3}); ρ is the density of saline aquifer water (ML^{-3}); and Z is the midpoint elevation below sea level for each layer (L).

$$h_f = \frac{\rho}{\rho_f} h - \frac{\rho - \rho_f}{\rho_f} Z \tag{8}$$

Taking the model depth as 100 m and placing the proper parameters in the equation, coastal boundary hydraulic head was calculated as 1.25 m.

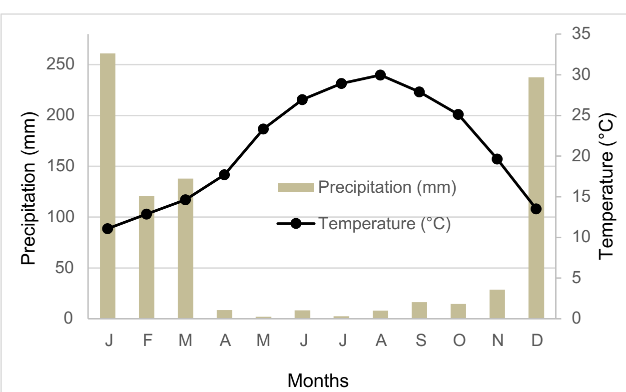

Fig. 6 Monthly total precipitation amount (mm) and monthly mean temperature data (°C) in Mersin for the year of 2019

Model parameters and recharge

The effect of heterogeneity on ATES well efficiency has been studied by Caljé (2010), Sommer et al. (2013), Possemiers et al.

(2015), and Xynogalou (2015), who concluded that only in specific conditions heterogeneity may have a significant effect. Therefore, physical properties such as horizontal and vertical hydraulic conductivity, porosity, and bulk density of each stratigraphic unit were taken as homogeneous. Different data sources in the literature have been used to determine the horizontal and vertical hydraulic conductivity of each soil type in the model that constitute the model layers (Bridger and Allen 2010; Banks 2012; Craig 2004). As hydraulic conductivity has negligible effects on thermal losses under homogeneous and nonbuoyant flow (Bloemendal and Hartog 2018), the horizontal hydraulic conductivities for each layer were set to the constant values. The vertical hydraulic conductivity distribution for each soil layer was assumed to obey the vertical to horizontal hydraulic conductivity ratio (K_z/K_h) of 0.1 (e.g., Todd 1980). Porosity and bulk density parameters are taken based on the available values in the literature and are given in Table 1.

Precipitation values constitute the recharge data of the groundwater flow model. The net precipitation, given in Eq. (9), is the difference between the measured precipitation minus evapotranspiration (ETP). Total annual precipitation values for the year of 2019 were calculated with the information gathered from Mersin Meteorology Service (Fig. 6). Annual evaporation losses were determined by the Turc method (Turc 1954) given in Eq. (10) using the annual total precipitation and average temperature values. The N parameter is a coefficient depending on the average temperature defined as $N = A + 25T + 0.05T^3$. Here, A is a basin-specific coefficient that varies between 0 and 300 based on the data derived for all the river basins in Turkey (Ozer 1990). This parameter was determined as 300 for the coastal region of Mersin province. The well module of the MODFLOW software is used to introduce the irrigation wells to the hydrogeological model.

$$Q = P - \mathrm{ETP} \tag{9}$$

$$\mathrm{ETP} = \frac{P}{\sqrt{0.9 + \left(\frac{P}{N}\right)^2}} \tag{10}$$

where ETP is evapotranspiration (mm); P is total precipitation (mm); T is the annual mean temperature (C°); and Q is the estimated annual mean net recharge (mm). ETP and Q values are calculated as 699.31 mm and 147.19 mm, respectively.

Steady-state calibration of the groundwater flow model

The coordinates of the well locations at various points of the study area and the measured groundwater levels were introduced to the overall model through wells module. Names, coordinates of the observation wells, pumping rate for each soil layer, and groundwater levels were defined to the system as input parameters. The model was run under steady-state conditions to simulate one year period between 2018 and 2019. The preconditioning conjugate gradient (PCG2) solution scheme was used. The number of allowed external and internal iterations in the PCG2 package was set to 50 and 30, respectively, and maximum tolerated value of 0.01 was taken as the convergence criterion, which is the maximum hydraulic level change between two consecutive iterations. Iterations stop when the maximum hydraulic level change between two consecutive iterations is smaller than the convergence criterion specified in the model.

The calibration of the hydrogeological model is based on the comparison of the actual groundwater levels with the groundwater levels predicted by the model. MODFLOW compares the observed and calculated groundwater levels of the observation wells and shows the statistical relationship between them. To improve the match between observed and simulated heads, horizontal and vertical hydraulic conductivity values were changed for the soil layers in the model. As seen in Fig. 7, a good fit was obtained between the observed and simulated heads. The difference between the groundwater levels calculated with the numerical model and the observed groundwater levels ranged from −0.24 to +0.40 m with a mean difference of 0.06 m and a standard deviation of 0.20 m. Groundwater level contours calibrated for the steady-state flow conditions were depicted in Fig. 8. Calibrated model revealed that the groundwater flows from the northwest direction to the southeast direction. Hydraulic gradients are calculated as 0.3180 % in the northwest regions where the hydraulic head contours are close to each other and 0.0012 % in the

Table 1 Parameters used in groundwater flow model

Stratigraphic unit	Horizontal hydraulic conductivity (m/day)[a]	Vertical hydraulic conductivity (m/day)[b]	Porosity	Bulk density (kg/m^3)
Layer 1 (clay)	1.60	0.16	0.20	1600
Layer 2 (gravel)	25.00	2.50	0.35	1800
Layer 3 (gravelly clay)	16.00	1.60	0.20	1600

[a] Based on values Bridger and Allen (2010), Banks (2012), and Craig (2004)

[b] (K_z/K_h) was assumed to be 0.1 (Todd 1980)

Table 2 Water budget of the numerical groundwater flow model

Flow term	In (m^3/day)	In (%)	Out (m^3/day)	Out (%)	In-Out (m^3/day)
Constant head	2226	86	2439	94	−213
Wells	0.00	–	148	6	−148
Recharge	361	14	0.00	–	361
River	0.00	–	0.00	–	0.00
Total	2587	100.00	2587	100.00	0.00
Discrepancy (%)	0.00	0.00	0.00	0.00	0.00

southeast regions close to the sea. Water budget of the numerical groundwater flow model for one year period is shown in Table 2. As expected from a steady-state model, the water budget shows a good balance between inflows and outflows.

Initial design calculations of conceptual ATES system

Current experience with ATES systems has shown that the presence of a suitable aquifer for groundwater supply and energy storage is the main factor determining the feasibility of an ATES system (Hall and Raymond 1992). Heterogeneous aquifer conditions have been shown as a key factor influencing thermal plume movement and energy recovery in ATES systems (Tsang et al. 1981; Buscheck et al. 1983; Molz et al. 1983; Xue et al. 1990). In simple geologic settings, simplified representations of aquifers in heat transport models may not be unreasonable; however, in settings where heterogeneous conditions exist, such oversimplifications may lead to unrealistic design. To be able to overcome this problem, thermo-hydraulic model of this study has been coupled with a detailed groundwater flow model taking the

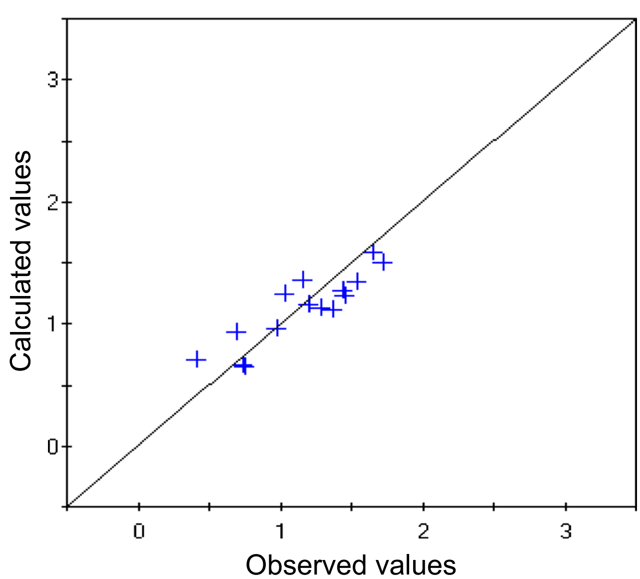

Fig. 7 Comparison of the simulated and measured actual groundwater head in the coastal aquifer

heterogeneous topographic conditions, hydrogeological parameters, and boundary conditions into account. The heat transfer model for the conceptual ATES system was set using fixed injection temperatures and equal injection and extraction rates (Q), i.e., a closed water volume balance. During the analyses, injection temperatures were set to 25 °C. Contrary to the standard ATES applications, continuous operational regime (Fig. 9) was modelled to be able to make solid comparisons between the analytical and finite difference model results. The initial aquifer temperature was fixed at 20 °C throughout the whole model domain based on the actual groundwater temperature values. The temperature differences due to thermal storage are small enough to neglect the temperature dependency of density and viscosity (Bridger and Allen 2010; Fossoul et al. 2011; Zuurbier et al. 2013). Bear (1972), Ingetbritsen and Sanford (1998), and Hopmans et al. (2002) have concluded that the effects of thermal dispersion are negligible and should be set to zero. As such, thermo-hydraulic model sensitivity was evaluated with the dispersion values set to zero.

Groundwater flow control is an important criterion in the design of ATES projects. Ensuring the continuity of high abstraction pressure in all operating conditions that occur due to seasonal temperature changes is one of the major factors ruling the design of the system. In particular, as a result of the incorrect design of the injection well, clogging by fine particles or chemical precipitates may occur over time and the recharge well performance may decrease. Injection wells are more susceptible to clogging and degradation as compared to abstraction wells. In the abstraction wells, water is pumped out of the aquifer and there will be some amount of self-cleaning tendency. In the injection wells, water is forced into the aquifer and any well screen; if the re-injected water contains any particles or chemical precipitates, these can lodge in the well screen or aquifer pore spaces thus reducing their permeability. Hence, proper design of injection wells require more technical effort. The highest allowable injection velocity, $v_{\mathrm{injection}}$ (m/h) for well screens that limits the clogging is expressed by Eq. (11) suggested by Buik and Snijders (2012). In this equation, K denotes the hydraulic conductivity of the geological unit (m/day); v_{cl} is the specific clogging rate

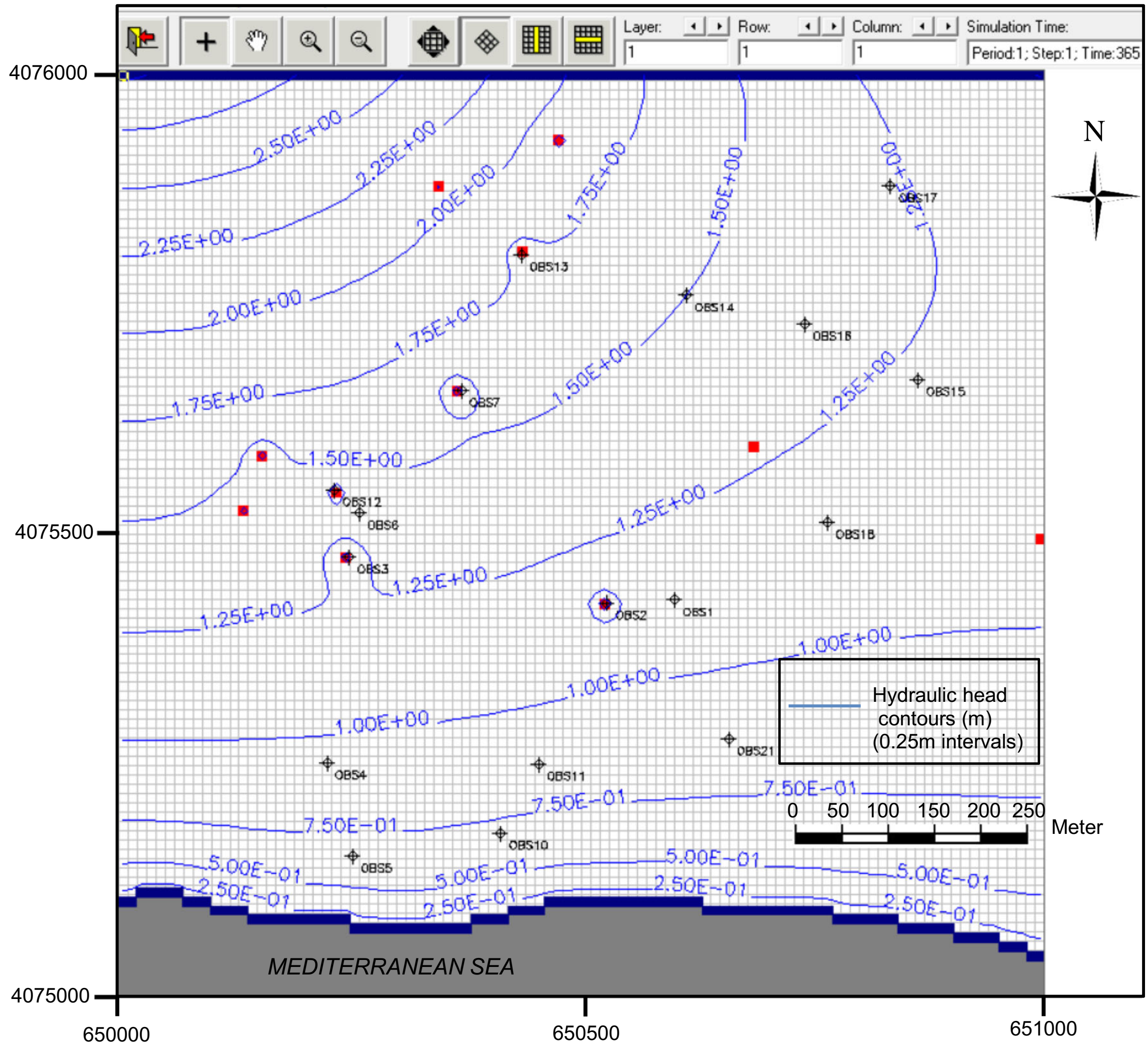

Fig. 8 Distribution of simulated hydraulic head contours after calibration

(m/year); MFI is the membrane filter index (s/l^2) depending on the well filter type, and u_f denotes the equivalent full load operating hours. In addition, the design extraction Darcy velocity on the borehole walls is expressed by Eq. (12) suggested by IF Technology (2001) and NVOE (2006). The lower of the abstraction and injection well velocities is considered to be the design velocity, v_{design} (m/h), which determines the

Fig. 9 A sketch depicting the continuous operational regime for aquifer thermal energy storage (adopted from Lee 2010) to be used in thermo-hydraulic modeling phase

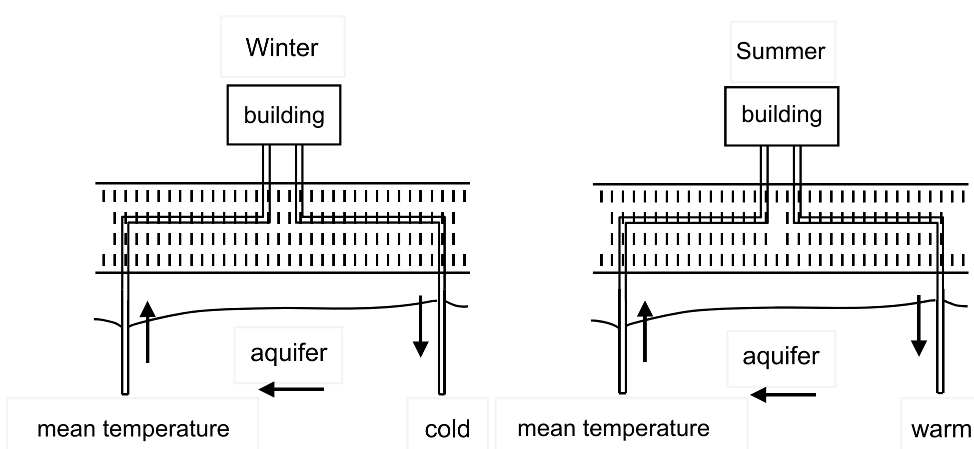

velocity on the walls of the borehole. The flow rate (m^3/h) of the ATES well is determined according to the design velocity limiting the well clogging problem and can be calculated using Eq. (13) (Groot 2013). In this equation, r_0 refers to the well diameter (m) and H refers to the well filter depth (m).

$$v_{\text{injection}} = 1000\left(\frac{K}{150}\right)^{0.6}\sqrt{\frac{v_{\text{cl}}}{2(\text{MFI})u_{\text{eq}}}} \tag{11}$$

$$v_{\text{extract}} = \frac{K_s}{12} \tag{12}$$

$$v_{\text{design}} = \frac{Q_{\text{inf,ex}}}{2\pi r_0 H} \tag{13}$$

For the initial design of the conceptual ATES system, the methods carried out in the Netherlands for the determination of the abstraction/injection rate that limits the clogging specified by Groot (2013) were followed in this study. The design velocity on the well walls with a diameter of 20 cm was calculated for the worst scenario. Taking specific clogging rate as 0.1m/year, MFI value as 2 s/l^2 and equivalent full load operating time as 2400 h (NVOE 2006; Tauw 2008) for K = 25m/day, injection and abstraction velocities were calculated as 1.10 m/h and 2.08 m/h, respectively. The design velocity of the borehole wall, v_{design}, was accepted as 1.00 m/h. The allowable groundwater discharge that can be abstracted from the aquifer thermal storage without clogging the well screens and injected back into the aquifer with the continuous operation of the system for a whole day was calculated as 715 m^3/day. However, the flow rate for a well to be drilled along the full depth of the aquifer is taken as 4 l/s that is 345.6 m^3/day in this study.

Thermo-hydraulic model

Initial and boundary conditions and model parameters

Heat transport simulations were carried out by assigning thermal boundary conditions and thermal parameters to the groundwater flow model for the target coastal aquifer. The underground heat transfer is modeled using the MT3DMS (Modular Transport 3-D Multi-Species) add-on module, which can be integrated into the MODFLOW software (Zheng and Wang 1999). In subsoil heat convection models, the integration of boundary conditions into the code is performed using the ICBUND array similar to groundwater flow models. In the ICBUND scheme, active cells with changing temperature are defined as positive, cells with constant temperature as negative, and inactive cells where heat transfer does not occur, as zero. In this study, the north and south boundaries of the model were defined as the constant temperature boundary, east and west boundaries of the model and the other cells in the study area were entered as active cells, whereas the cells located south of the coastal border were assigned as inactive cells. As the initial temperature values in the whole model, average groundwater temperatures that were obtained from the measurements performed at the wells in the study site were taken. Considering the temperature data, the initial temperatures were entered to the model as 20 °C (293.15°K). The initial temperature values are introduced to the model as constant and same for each cell of the model similar to other ATES modeling studies (Caljé 2010). The parameters used in the calibration of the thermo-hydraulic model are given in Table 3. Thermal conductivity values (λ_s) and specific heat capacity values (c_s) of each layer were obtained from (Caljé 2010). Bear (1972), Ingetbritsen and Sanford (1998), and Hopmans et al. (2002) have concluded that the effects of thermal dispersion are negligible and should be set to zero in the analyses. Therefore, the effect of the dispersive heat transport was neglected in the model.

Calibration of the heat transport model

Method of characteristics (MOC) was chosen at the stage of running the thermo-hydraulic model which is widely used in the solution of advective transport in solute transport models. One of the most advantageous aspects of this method used in solute transport simulations, where advection is more effective than dispersion, is that less numerical rounding error occurs during numerical calculations compared to other advection solution methods (Zheng and Wang 1999). The biggest disadvantage of the MOC method is considered as the computation time takes longer than other methods and the calculated concentrations sometimes tend to show artificial oscillations. The Courant number determined in this method represents the number of cells a particle will be allowed to move in any direction during the advection step of mass transport simulations. The Courant number, which describes the number of cells an average particle will travel through per unit time, usually takes a value between 0.5 and 1.0. In the thermo-hydraulic model, the Courant number was taken as 0.75 and the temperature values calculated by the model were calibrated by comparing them with analytical methods.

The duration of the thermal breakthrough resulting from the continuous operation of the injection well (located at grid coordinate i =23, j=40) and the extraction well (located at grid coordinate i=29, j=48) placed at a distance of 100 m from each other parallel to the groundwater flow direction (Fig. 10) was compared with the thermal breakthrough time calculated using Eq. (6) suggested by Banks (2012). In order to compare the temperature values calculated by analytical methods and the numerical simulations, thermo-hydraulic model was set on

Table 3 Thermo-hydraulic model parameters

Model parameters	Unit	Layer 1 (clay)	Layer 2 (gravel)	Layer 3 (gravelly clay)
Solid thermal conductivity (λ_s) [a]	(W/m/K)	1.70	2.50	1.70
Porosity (n)	(–)	0.20	0.35	0.20
Effective thermal conductivity of the porous media ($\lambda_m=\lambda_f^{\,n}+\lambda_s^{(1-n)}$)	(W/m/K)	2.42	2.64	2.42
Density of the solid material (=minerals) (ρ_s)	(kg/m^3)	2000	2770	2000
Dry bulk density ($\rho_b=(1-n)\rho_s$)	(kg/m^3)	1600	1800	1600
Specific heat capacity of the solid (c_s)[a]	(J/kg/s)	1000	920	1000
Specific heat capacity of the porous medium ($c_m=c_f n+(1-n)c_s$)	(J/kg/s)	1636	2061	1636
Distribution coefficient ($K_d=c_s/\rho_w c_w$)	(m^3/kg)	2.40×10^{-4}	2.20×10^{-4}	2.40×10^{-4}
Specific heat capacity of the water (c_f)	(J/m^3/s)	4180	–	–
Water thermal conductivity (λ_f)	(W/m/K)	0.58	–	–
Density of water (ρ_w)	(kg/m^3)	1000	–	–
Undisturbed temperature of the ground	(K)	293.15	–	–

[a] Values from Caljé (2010)

the basis of the assumptions made in the analytical thermal breakthrough equation. For this purpose, the filters of the well doublet placed parallel to the groundwater flow direction were defined in the model along the full depth of the aquifer (23.73 m) and it was assumed that the effect of the dispersive heat transport was neglected in the model. Moreover, groundwater at 25 °C was continuously injected into the aquifer unlike the cyclic working principle of ATES systems. Flow rate for the

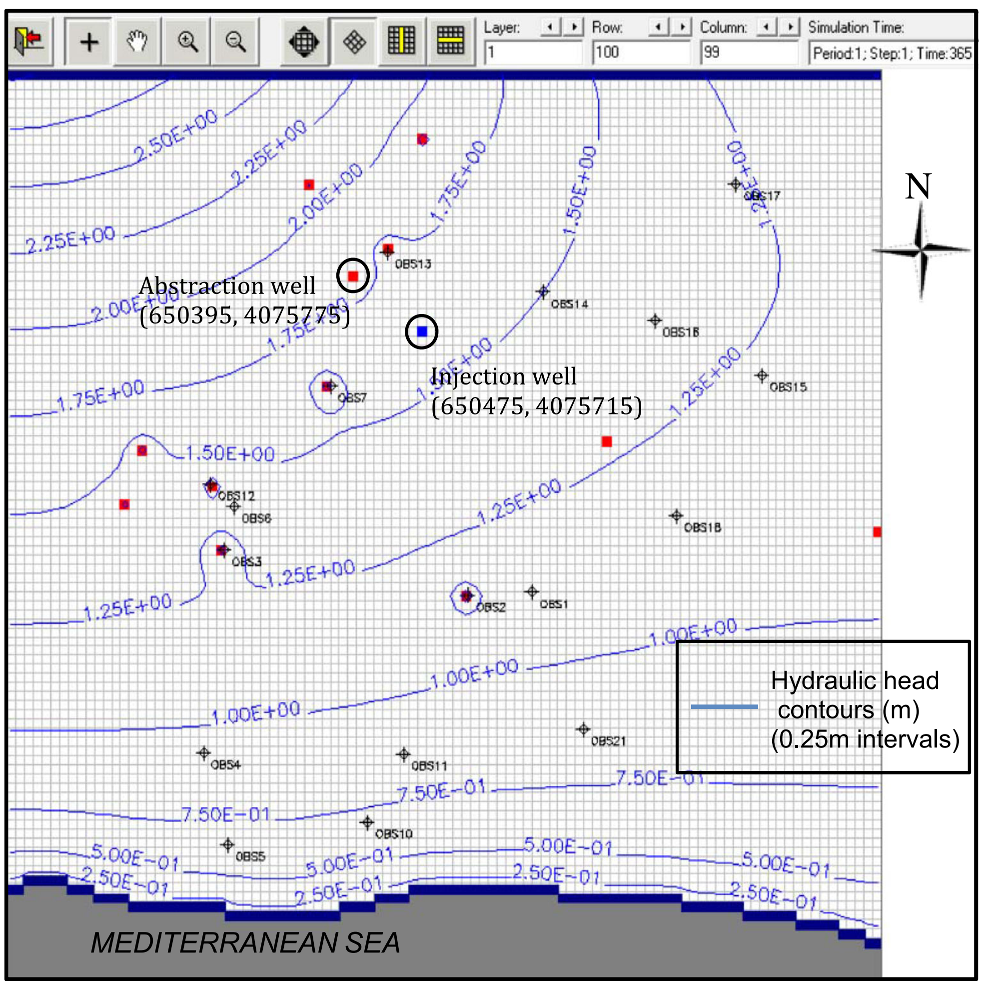

Fig. 10 Location of the abstraction and injection wells in thermo-hydraulic modeling phase

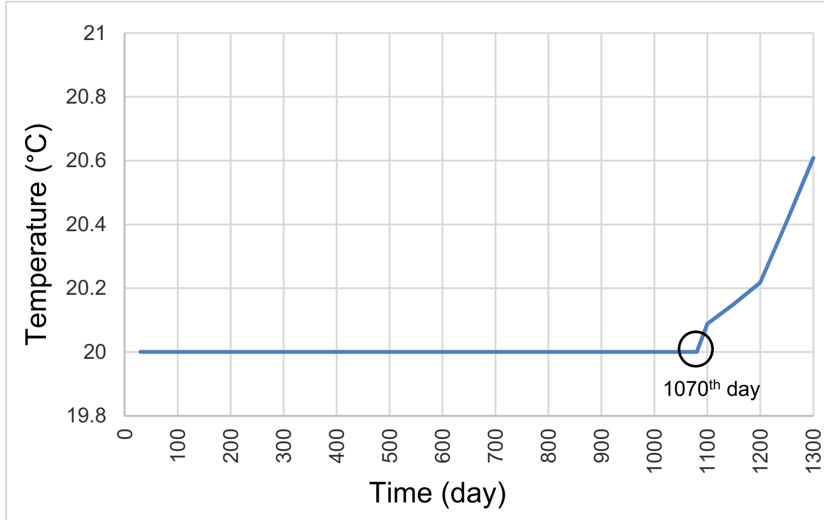

Fig. 11 Simulated temperature (°C) values of the abstraction well changing with time indicating the thermal interaction

MT3DMS is taken as 345 m^3 per day which is the limiting value for the clogging risk of the abstraction and injection wells. The additional parameters defined in Table 3 were introduced to the thermo-hydraulic model. Analyses results showed that the groundwater temperatures observed in the abstraction well started to increase dramatically by the 1070th day, affected by the heat dissipation of the warm groundwater stored in the injection well as depicted in Fig. 11. In the thermo-hydraulic model, the heat energy dissipation stored in the injection well and the beginning of the thermal interactions occurring between the abstraction and injection wells on the 1070th day are shown in Fig. 12. In this figure,

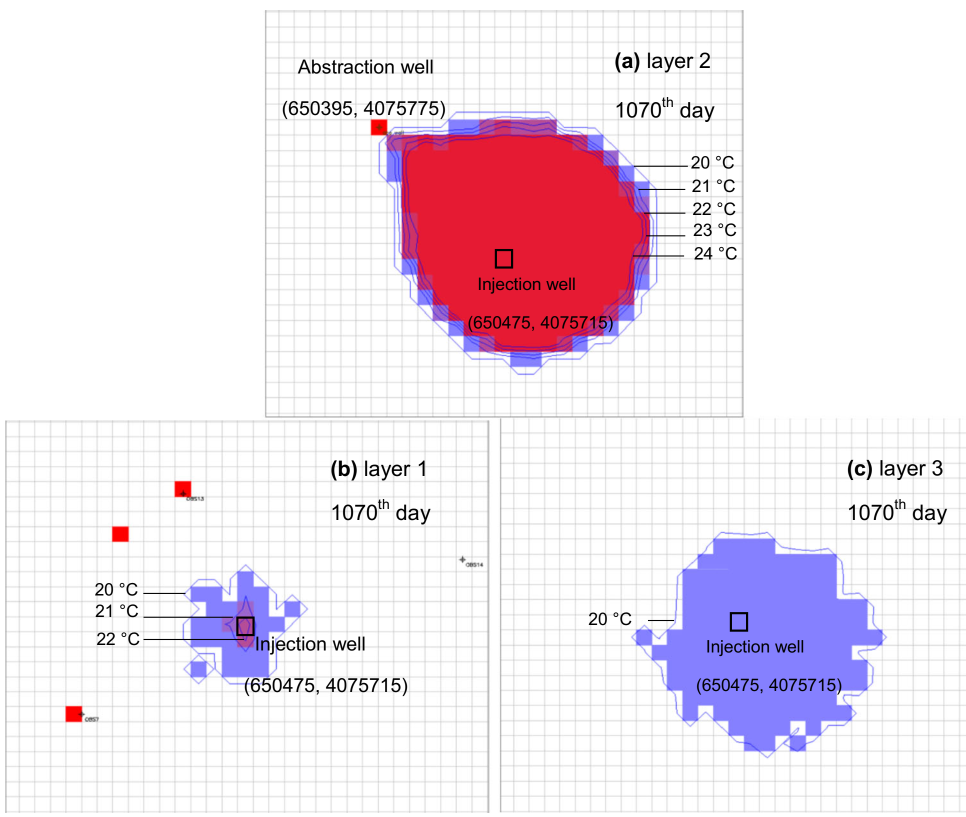

Fig. 12 Thermal interactions between abstraction and injection wells on 1070th day: **a** layer 2 that the thermal energy is stored, and (**b**, **c**) layers 1 and 3, respectively, indicating the heat fluxes through the upper and lower strata

thermal plume of the injection well within the layer 2 (a) and the heat migration via conductive processes into overlying and underlying layers (b) and (c), respectively, on the 1070th day are presented.

In order to compare the thermo-hydraulic model results with those obtained by analytical solution, the parameters of the model were used in the thermal breakthrough time equation given in Eq. (7). The natural hydraulic gradient between the wells was calculated as $i = 0.2064\%$ to be used in the calculation of the β coefficient with Eq. (5). This coefficient was obtained as 1.633 and accordingly thermal breakthrough time obtained with the analytical solution was calculated as 887 days. The discrepancy of the results of the thermal breakthrough time calculated by the analytical method and numerical model is due to the reason that groundwater flow and heat transfer are two-dimensional and restricted to the horizontal plane by the analytical solution. However, this is not true for heat as the heat can be transferred by conduction into underlying rocks and towards the surface via overlying soil layers. This means that any thermal plume or thermal feedback is attenuated much more rapidly that the model would suggest. In other words, the two-dimensional analytical method is rather conservative (Banks 2015) when compared to reality (Fig. 3b). Although there is a difference between the analytical and three-dimensional thermo-hydraulic model results in terms of thermal breakthrough time, it was observed that the thermal breakthrough time that was obtained by the analytical formula and the value predicted by thermo-hydraulic model are close to each other revealing that well-calibrated numerical model can realistically represent the thermal behavior in the field.

Conclusions

In this study, results of numerical simulations that were performed to optimize and determine the sustainable development and utilization plan for a conceptual open-loop ground source heating well doublet in a regional groundwater flow field which will be built in a coastal aquifer in Turkey were presented. Within this scope, simulations for the heat transfer scheme and the thermal response for the coastal aquifer are performed by an extensive numerical modeling study. In the first phase, a three-dimensional numerical groundwater flow model taking the heterogeneities into account was produced. Calibrated hydrogeological model revealed that the groundwater flows from the northwest direction to the southeast direction in the study area. Consequently, heat transfer regime of the coastal aquifer was performed by coupling thermal model with hydrogeological model. An approach was suggested for the numerical model calibration by comparing the aquifer temperature values predicted by the finite difference thermo-hydraulic model with those of the analytical solutions. Although the two-dimensional analytical model do not take the possibility for heat to migrate via conductive processes into overlying and underlying strata into account and therefore rather conservative when compared with 3D finite-element numerical modelling, results of this study indicated that a reasonably good fit is present in thermal breakthrough from an operational perspective of an ATES system. The approach for the numerical model calibration by comparing the aquifer temperature values estimated by the finite difference thermo-hydraulic model with those of the analytical solution suggested in this paper can be considered as an effective, simpler, and faster way for the pre-feasibility and initial design procedure for the low-temperature aquifer thermal energy storage systems. The presented methodology is suitable for use in modeling similar ATES systems and may significantly decrease the amount of on-site tests that should be performed to estimate the working parameters of an anticipated thermal energy storage system.

Acknowledgements The authors would like to thank to all reviewers for their critical reviews and comments that improved the manuscript.

Declarations

Conflict of interests The authors declare no competing interests.

References

Anderson MP (2005) Heat as a ground water tracer. Groundwater 43(6): 951–968

Andersson O, Hellstrom G, Nordell B (2003) Heating and cooling with UTES in Sweden: current situation and potential market development. In:International Conference on Thermal Energy Storage: 01/09/2003-04/09/2003 (pp. 207-215). PW Publishing House

Banks D (2011) The application of analytical solutions to the thermal plume from a well doublet ground source heating/cooling scheme. Q J Eng Geol Hydrogeol 44:191–197

Banks D (2012) An introduction to thermogeology: ground source heating and cooling, 2nd edn. Wiley, Blackwell Publication, Oxford

Banks D (2015) A review of the importance of regional groundwater advection for ground heat exchange. Environ Earth Sci 73(6): 2555–2565

Bear J (1972) Dynamics of fluids in porous media. American Elsevier Publishing Company Inc., New York

Bear J (1979) Hydraulics of groundwater. McGraw-Hill, USA, New York

Bloemendal JM (2018) The hidden side of cities: methods for governance, planning and design for optimal use of subsurface space with ATES. Delft University of Technology, Dissertation

Bloemendal M, Hartog N (2018) Analysis of the impact of storage conditions on the thermal recovery efficiency of low-temperature ATES systems. Geothermics 17:306–319

Bloemendal M, Olsthoorn T, Van de Ven F (2015) Combining climatic and geo-hydrologic preconditions as a method to determine world potential for aquifer thermal energy storage. Sci Total Environ 538: 621–633

Bridger DW, Allen DM (2005) Designing aquifer thermal energy storage systems. ASHRAE J 47(9):32

Bridger DW, Allen DM (2010) Heat transport simulations in a heterogeneous aquifer used for aquifer thermal energy storage (ATES). Can Geotech J 47(1):96–115

Buik NA, Snijders AL (2012) Clogging of recharge wells in porous media. MEDIA. https://intraweb, stockton. edu/eyos/energy studies/content/docs/FINAL_PAPERS A, 13
Buscheck TA, Doughty C, Tsang CF (1983) Prediction and analysis of a field experiment on a multilayered aquifer thermal energy storage system with strong buoyancy flow. Water Resour Res 19(5):1307–1315. https://doi.org/10.1029/WR019i005p01307
Cabeza LF, Miró L, Oró E, de Gracia A, Martin V, Krönauer A, Rathgeber C, Farid MM, Paksoy HO, Martínez M, Fernández AI (2015) CO2 mitigation accounting for thermal energy storage (TES) case studies. Appl Energy 155:365–377
Caljé R (2010) Future use of aquifer thermal energy storage in below the historic centre of Amsterdam. Delft University of Technology, Dissertation
Cetin A, Apaydin A, Paksoy HO (2012) Yeraltısuyu Termal Enerjisinin Isıtma ve Soğutmada Kullanımı: Avrupa ve Türkiye'deki Durumun teknik ve Yasal Yönleriyle Değerlendirilmesi. DSI Teknik Bulteni 128:22–36
Cetin A, Kadioglu YK, Paksoy HO (2020) Underground thermal heat storage and ground source heat pump activities in Turkey. Sol Energy 200:22–28
Clyde CG, Madabhushi GV (1983) Spacing of wells for heat pumps. J Water Resour Plan Manag 109(3):203–212
Craig RF (2004) Craig's soil mechanics. CRC press, Boca Raton
De Marsily G (1986) Quantitative hydrogeology: groundwater hydrology for engineers. Academic Press, New York
Dickinson JS, Buik N, Matthews MC, Snijders A (2009) Aquifer thermal energy: theoretical and operational analysis. Geotechnique 59(3): 249–260
Doughty C, Hellstrom G, Tsang CF (1982) A dimensionless approach to the thermal behavior of an aquifer thermal energy storage system. Water Resour Res 18(3):571–587
Fleuchaus P, Godschalk B, Stober I, Blum P (2018) Worldwide application of aquifer thermal energy storage–a review. Renew Sust Energ Rev 94:861–876
Fossoul F, Orban P, Dassargues A (2011) Numerical simulation of heat transfer associated with low enthalpy geothermal pumping in an alluvial aquifer. Geol Belg 14(1–2):45–54
Gao L, Zhao J, An Q, Wang J, Liu X (2017) A review on system performance studies of aquifer thermal energy storage. Energy Procedia 142:3537–3545
Groot J (2013) Optimizing energy storage and reproduction for aquifer thermal energy storage. University Utrecht, Dissertation
Hall SJ, Raymond JR (1992) Geohydrologic characterization for aquifer thermal energy storage. In Proceedings of the Intersociety Energy Conversion Engineering Conference, San Diego, Calif 75–81
Harbaugh AW, Banta ER, Hill MC and McDonald MG (2000) MODFLOW-2000, the U.S. geological survey modular groundwater model-user guide to modularization concepts and the ground-water flow process. Open-file report, U.S. Geol Surv (92): 134
Hatipoglu-Bagci Z (2004)Mersin-Tarsus kıyı akiferinin hidrojeokimyası. Mersin University, Dissertation
Hatipoglu-Bagci Z, Bayari CS, Canakci A, (2019) CrVI contaminated groundwater in the Mediterranean: case study from Mersin, Turkey, 16th International Conference on Environmental Science and Technology, Rhodes, Greece, 4-7 September 2019
Hecht-Méndez J, Molina-Giraldo N, Blum P, Bayer P (2010) Use of MT3DMS for heat transport simulation of shallow geothermal systems. In:World Geothermal Congress 1-8
Hopmans JW, Simunek J, Bristow KL (2002) Indirect estimation of soil thermal properties and water flux using heat pulse probe measurements: geometry and dispersion effects. Water Resour Res 38(1):7–1
IF Technology (2001) Ontwerpnormen voor bronnen voor koude-/warmteopslag (Design criteria for ATES wells; in Dutch). Research project, project reference 149.508-105.0. Arnhem, Netherlands
Ingetbritsen SE, Sanford WE (1998) Groundwater in geologic processes. Cambridge University Press, Cambridge
Kim J, Lee Y, Yoon WS, Jeon JS, Koo MH, Keehm Y (2010) Numerical modeling of aquifer thermal energy storage system. Energy 35: 4955–4965
Kranz S, Frick S (2013) Efficient cooling energy supply with aquifer thermal energy storages. Appl Energy 109:321–327
Lee KS (2010) A review on concepts, applications, and models of aquifer thermal energy storage systems. Energies 3(6):1320–1334
Lee KS (2013) Underground thermal energy storage. Springer, London
Molz FJ, Melville JG, Parr AD, King DA, Hoff MT (1983) Aquifer thermal energy storage: a well doublet experiment at increased temperatures. Water Resour Res 19(1):149–160. https://doi.org/10.1029/WR019i001p00149
Novo AV, Bayon JR, Castro-Fresno D, Rodriguez-Hernandez J (2010) Review of seasonal heat storage in large basins: water tanks and gravel–water pits. Appl Energy 87(2):390–397
NVOE (2006) Nederlandse Vereniging voor Ondergrondse Energieopslagsystemen-Richtlijnen Ondergrondse Energieopslag (Dutch Association for Underground Energy Storage Systems-Guidelines for Underground Energy Storage). Woerden, Netherlands
Ozer Z (1990) Su yapılarının projelendirilmesinde hidrolojik ve hidrolik esaslar. Tarım Orman ve Köy İşleri Bakanlığı Köy Hizmetleri Genel Müdürlüğü. Havza Islahı ve Göletler Daire Başkanlığı, Ankara
Possemiers M, Huysmans M, Batelaan O (2015) Application of multiple-point geostatistics to simulate the effect of small-scale aquifer heterogeneity on the efficiency of aquifer thermal energy storage. Hydrogeol J 23(5):971–981
Preene M, Powrie W (2009) Ground energy systems: delivering the potential. Energy 162(2):77–84
Rafferty K (2003) Ground water issues in geothermal heat pump systems. Ground Water 41(4):408–410
Rosen MA (1999)Second-law analysis of aquifer thermal energy storage systems. Energy 24(2):167–182
Rostampour V, Bloemendal M, Jaxa-Rozen M, Keviczky T (2016) A control-oriented model for combined building climate comfort and aquifer thermal energy storage system, in: Proceedings European Geothermal Congress, Strasbourg
Sanner B (2001) Shallow geothermal energy. GHC Bull 19-25
Schüppler S, Fleuchaus P, Blum P (2019)Techno-economic and environmental analysis of an aquifer thermal energy storage (ATES) in Germany. Geotherm Energy 7(1):1–24
Sommer WT, Valstar J, van Gaans P, Grotenhuis T, Rijnaarts H (2013) The impact of aquifer heterogeneity on the performance of aquifer thermal energy storage. Water Resour Res 49(12):8128–8138
Sommer W, Valstar J, Leusbrock I, Grotenhuis T, Rijnaarts H (2015) Optimization and spatial pattern of large-scale aquifer thermal energy storage. Appl Energy 137:322–337
Tauw (2008)Warmte-Koudeopslag Achmea te Apeldoorn. Final design, 30 July 2009
Todd DK (1980) Groundwater hydrology. Wiley, New York
Tsang CF, Buscheck T, Doughty C (1981) Aquifer thermal energy storage: a numerical simulation of Auburn University field experiments. Water Resour Res 17(3):647–658. https://doi.org/10.1029/WR017i003p00647
Turc L (1954) Le bilan d'eau des sols: relations entre les precipitations, l'evaporation et l'ecoulement (Ground water variations: relations between precipitations, evaporation and runoff). J de l'Hydraulique 3(1):36–44
Xue Y, Xie C, Li Q (1990) Aquifer thermal energy storage: a numerical simulation of field experiments in China. Water Resour Res 26(10): 2365–2375

Xynogalou M (2015) Determination of optimal separation well distance for single borehole ATES systems in the Netherlands, implementing an axisymmetric numerical model. Delft University of Technology, Dissertation

Zheng C, Wang P (1999) MT3DMS: a modular three-dimensional multispecies transport model for simulation of advection, dispersion, and chemical reactions of contaminants in groundwater systems: documentation and user's guide. US Army Corps of Eng

Zuurbier KG, Hartog N, Valstar J, Post VE, van Breukelen BM (2013) The impact of low-temperature seasonal aquifer thermal energy storage (SATES) systems on chlorinated solvent contaminated groundwater: modeling of spreading and degradation. J Contam Hydrol 147:1–13